

1 **Systemic enrichment of antifungal traits in the rhizosphere microbiome after pathogen attack**

2

3 Jan-Hendrik Dudenhöffer^{1*}, Stefan Scheu², Alexandre Jousset³

4

5 ¹Department of Nature Conservation and Landscape Ecology, Institute of Earth and Environmental
6 Sciences, University of Freiburg, Tennenbacher Straße 4, 79106 Freiburg, Germany.

7 ²Animal Ecology, J. F. Blumenbach Institute of Zoology and Anthropology, Georg August University
8 Göttingen, Berliner Straße 28, 37073 Göttingen, Germany

9 ³Utrecht University, Ecology and Biodiversity, Padualaan 8, 3584CH Utrecht, The Netherlands.

10

11 *Corresponding author: jan.dudenhoeffer@nature.uni-freiburg.de; Phone: +49 761 203 8655

12

13 **Running headline:** *Recruitment of beneficial microbes*

14 **Summary**

15
16 **1.** Plant-associated microbial communities are crucial for plant growth and play an important role in
17 disease suppression. Community composition and function change upon pathogen attack, yet to date we
18 do not know if these changes are a side effect of the infection or actively driven by the plant.

19 **2.** Here we used a split-root approach to test whether barley plants recruit bacteria carrying antifungal
20 traits upon infestation with *Fusarium graminearum*. Split-root systems allow disentangling local infection
21 effects, such as root damage, from systemic, plant-driven effects on microbiome functionality. We
22 assessed the recruitment of fluorescent pseudomonads, a taxon correlated with disease suppression, and of
23 two well-described antifungal genes (*phlD* coding for 2,4-DAPG and *hcnAB* coding for HCN).

24 **3.** We show an enrichment of fluorescent pseudomonads, *phlD* and *hcnAB* upon pathogen infection. This
25 effect was only measurable in the uninfected root compartment. We link these effects to an increased
26 chemotaxis of pseudomonads towards exudates of infected plants.

27 **4. Synthesis.** We conclude that barley plants selectively recruited bacteria carrying antifungal traits upon
28 pathogen attack and that the pathogen application locally interfered with this process. By disentangling
29 these two effects we set the base for enhancing strategies unravelling how pathogens and plant hosts
30 jointly shape microbiome functionality.

31

32 **Key words:**

33 Barley, *Fusarium graminearum*, Plant-microbe interactions, *Pseudomonas*, Recruitment, Split-root

34

35 **Introduction**

36
37 Plant pathogens cause significant loss of agricultural yield worldwide (Strange & Scott 2005) and are an
38 important determinant of plant community structure and productivity (Packer & Clay 2000; Klironomos
39 2002; Van der Putten 2003; Petermann *et al.* 2008). Plant-associated microbes form a first line of defense
40 that may complement plant innate immunity. In particular the rhizosphere microbiome, the microbial
41 community associated with plant roots, is increasingly recognized to shape disease suppression
42 (Berendsen, Pieterse & Bakker 2012; Mendes *et al.* 2013).

43 The rhizosphere is a place of complex interactions between plants and microbes. Plants invest important
44 resources to secrete root exudates, a set of labile organic compounds able to recruit, feed and manipulate
45 the physiology of a subset of microbes present in the surrounding soil (Bais *et al.* 2006). In return several
46 of the associated microbes will protect plants against pathogens by producing antibiotics and stimulating
47 plant immunity (Bakker *et al.* 2013).

48 Plant microbiome composition varies as a function of plant identity and soil type (Costa *et al.* 2006; Aira
49 *et al.* 2010; Peiffer *et al.* 2013) and even with plant growth stage (Chaparro *et al.* 2013; Yuan *et al.* 2015),
50 indicating that the host plant exerts a structuring influence on the selection of microbial communities from
51 the available species pool. Also plant diseases play an important role and pathogen attack can be
52 associated with alterations in microbiome structure, functionality and activity (Trivedi *et al.* 2012).

53 These different effects interactively shape microbiome functionality in response to diseases, making it
54 hard to distinguish which changes are actively driven by the host plant (and thus indicate that a plant has
55 the ability to structure its microbiome) and which changes are self-assembly processes driven by changes
56 in the environmental conditions around the roots. Such passive changes encompass root damage by
57 pathogens, causing leaking of compounds, or an altered exudation in pathogen-challenged plants as a
58 result of a lower photosynthetic activity or a shunting of the nutrient flows toward healthy parts of the root
59 system (Henkes *et al.* 2011). However, there are several cues indicating that plants react to pathogen
60 infection by producing compounds that may attract and stimulate beneficial microbes (Rudrappa *et al.*

61 2008; Jousset *et al.* 2011). Such plant mediated processes might even favor specific functions if feedback
62 loops allow plants to reward microbes performing certain tasks, as reported for different plant-microbe
63 symbioses (Phillips *et al.* 2004; Kiers & Denison 2008).

64 In the present study we aim to disentangle pathogen- and plant-mediated effects on microbiome
65 functionality. To separate these effects we set up a split-root system with barley plants growing in a
66 natural soil. Split-root systems involve the separation of the root system into two hermetic compartments,
67 allowing plant-microbe interactions to be tracked independently. In the present case we added a fungal
68 pathogen to one of the compartments and measured alterations in functional traits of the root-associated
69 communities. At the treatment compartment, the pathogen may alter plant-microbe interactions by
70 preventing exudation or secreting mycotoxins (Henkes *et al.* 2011, Notz *et al.* 2002). In contrast, effects
71 observed on the systemic, non-infected compartments, can be safely attributed to plant-mediated effects
72 (Henkes *et al.* 2011; Jousset *et al.* 2011).

73 We specifically address whether 1) barley recruits different microbes upon pathogen infection, 2) whether
74 microbial recruitment is related to an enrichment of anti-fungal traits (functional genes) and 3) whether the
75 recruitment process contributes to the structuring of rhizosphere microbial communities. By combining
76 these aspects we aim to prove the concept that a host plant is able to manipulate its rhizosphere
77 microbiome structure to fit its functionality to the challenges, such as pathogen infection, that the plant is
78 facing.

79

80 **Methods**

81

82 *Study system*

83

84 We used a model system with barley (*Hordeum vulgare* L.) as host plant, *Fusarium graminearum*
85 (Schwabe) as fungal pathogen and fluorescent pseudomonads as potential pathogen antagonists. Barley is
86 the fourth most important cereal crop worldwide. It serves as food for animals and humans as well for

87 malt production (Newton *et al.* 2011) and its general root microbiome structure was recently examined
88 (Bulgarelli *et al.* 2015). One of its major pathogens, the soil-borne fungus *F. graminearum*, is responsible
89 for blight in cereals and a growing concern in agriculture (Goswami & Kistler 2004; Kazan, Gardiner &
90 Manners 2012). Especially its production of mycotoxins poses a serious threat to animal and human health
91 and makes contaminated products unusable (D’Mello, Placinta & Macdonald 1999).

92 In an earlier study Henkes *et al.* (2011) showed that the local infection of barley roots with *F.*
93 *graminearum* resulted in a reduction of carbon delivery to the infected root parts. An inoculation with
94 fluorescent pseudomonads (*P. protegens* CHA0) counteracted this effect and successfully prevented
95 barley biomass reduction due to the infection. In a further study Lanoue *et al.* (2010) showed that barley
96 plants changed their exudation profiles after root infection with *F. graminearum*. The plants responded
97 with the synthesis of organic acids exhibiting antifungal activity. Some of these compounds are also
98 known to trigger the production of antifungal metabolites by fluorescent pseudomonads (Jousset *et al.*
99 2011) and act as chemo-attractants for this bacterial taxon (Oku *et al.* 2014). Based on these evidences we
100 used this biological system as a model to test our concept that plants may actively manipulate their
101 rhizosphere microbiome in response to an external stressor.

102 Therefore, we set up two experiments using a split-root approach to disentangle plant- and pathogen
103 mediated effects on microbial communities. The two split-root systems consisted of two separated
104 compartments. One compartment was infected with the pathogen (hereafter the ‘treatment compartment’)
105 while the other compartment remained pathogen-free (hereafter the ‘systemic compartment’).

106

107 *Seedling preparation*

108

109 We used barley plants (*Hordeum vulgare* L. cv. ‘Barke’) grown from commercial seed material (Irnich
110 Inc., Frechen, Germany). Barley seeds were surface-sterilized as described previously (Henkes *et al.*
111 2011). Briefly, seeds were soaked in H₂SO₄ (62% v/v) for 1 h to remove glumes, washed two times in
112 sterile water and were surface-sterilized in AgNO₃ solution (2% w/v) for 20 min. AgNO₃ was removed by

113 five cycles of precipitation in 1% NaCl solution and washing in sterile water. Seeds were germinated on
114 3% water agar at 24 °C in darkness to check for contamination and to obtain roots big enough to be
115 transferred into the split-root systems. One three day old seedling was transferred into each split-root
116 microcosm and its roots were evenly separated to each of the compartments.

117

118 *Fungal inoculum*

119

120 We used *Fusarium graminearum* (Schwabe) strain FG17 as model pathogen. The fungal cultures were
121 maintained on potato dextrose agar (PDA, Carl Roth GmbH, Essen, Germany) in darkness. Prior to the
122 experimental application, we incubated a cube of actively growing culture of *F. graminearum* in sterile
123 sucrose solution (40g l⁻¹) for 7 days at room temperature on an orbital shaker at 40 rpm. The resulting
124 mycelium suspension was homogenized by placing it through a syringe and then repeatedly centrifuged at
125 2000 rpm for 2 min, rinsed five times with 0.1 x phosphate buffered solution (PBS) to remove nutrients
126 and finally adjusted to OD₆₀₀= 0.4 (optical density at 600 nm) in 0.1 x PBS. For the chemotaxis
127 experiment we used a spore suspension of the fungus. Therefore, an actively growing culture was
128 transferred to autoclaved mung bean medium (40 g of mung beans boiled in 1 l water for 20 min) and
129 incubated for 5 days at room temperature on an orbital shaker at 40 rpm. The resulting spore suspension
130 was repeatedly centrifuged at 3000 rpm for 5 min, rinsed five times with sterile water and finally adjusted
131 to OD₆₀₀= 0.1 in sterile water.

132

133 *Split root set up*

134

135 First, we assessed bacterial recruitment in a natural soil (hereafter ‘soil experiment’): We grew barley
136 plants in split-root microcosms made of a polypropylene base part, containing the compartment chambers,
137 (width: 78 mm, depth: 6 mm, height: 128 mm) and a polycarbonate cover plate. Before setting up, the
138 microcosms were autoclaved at 105 °C for 60 min. The compartment chambers were filled with non-

139 sterile soil from the field site of the Jena Experiment (see Müller, Scheu & Jousset 2013) and were
140 supplemented with 20% (w/w) sand to avoid soil clumping. Both compartments were irrigated separately
141 with sterile water via fiber-glass capillaries and had apertures on the top to allow for gas exchange (see
142 Fig. S1 in Supporting Information). After ten days growth at 20 °C and 12 h photoperiod under artificial
143 light ($120 \mu\text{mol m}^{-2} \text{s}^{-1}$), the treatment compartment of the split-root microcosms were inoculated with 4
144 ml of the mycelium suspension, spread evenly on the whole root system. The control plants received the
145 same amount of 0.1 x PBS.

146 Ten days after pathogen addition, the split-root systems were destructively sampled. Rhizosphere soil
147 samples were collected by gently removing the roots with adherent soil and suspended in 30 ml of 0.1 x
148 PBS on a horizontal shaker at 60 rpm for 30 min.

149 We chose the comparatively short growth period of ten days to allow the challenged plants to respond to
150 the pathogen while preventing too much infection damage which may have caused biases in the
151 interpretation.

152

153 *Microbial communities*

154

155 We followed changes in rhizosphere microbial communities at three levels: We assessed total bacterial
156 density as a marker for unspecific changes coming along with the infection, such as nutrient leaking,
157 affecting indiscriminately all microbes. Further we enumerated the density of fluorescent pseudomonads
158 as model group, which is consistently associated with disease suppression (Mendes *et al.* 2013) and the
159 specific antifungal genes *phlD* and *hcnAB* (as indicators for specific functional gene enrichment). Further,
160 we monitored the diversity of pseudomonads and their community structure to test for selective processes
161 structuring the rhizosphere.

162 In the second experiment (hereafter ‘the chemotaxis experiment’) we tested if exudates from infected
163 plants are chemo-attractant for bacteria with potential antifungal activity. Therefore, we used a gnotobiotic
164 system where the plants were confronted with the pathogen in otherwise sterile conditions. We built split-

165 root microcosms out of two sterilized 15 ml Falcon tubes (BD Biosciences, Heidelberg, Germany) filled
166 with sterile demineralized water.

167 Plants were grown for ten days at 20 °C and 12 h photoperiod after which we inoculated the treatment
168 compartment of half of the plants with 0.5 ml of fungal spore suspension or sterile water respectively.

169 After ten days, the water samples from the root compartments containing the root exudates, were filtered
170 through a 0.22 µm filter (Millipore, Merck, Darmstadt, Germany) to remove remaining fungal or root
171 particles and were stored at 4 °C until processing the chemotaxis assay.

172

173 *Culture based enumeration of bacteria – plate counts*

174

175 For the culture based enumeration of fluorescent pseudomonads and total heterotrophic bacteria, we
176 spread-plated the rhizosphere soil suspensions on Petri dishes with Gould's S1 medium (Gould *et al.*
177 1985) and R2A medium (Reasoner & Geldreich 1985) respectively. For plating on Gould's S1 medium
178 we used 50 µl of the 20 fold diluted suspensions and for R2A medium 50 µl of the 100 fold diluted
179 suspensions. Petri dishes were incubated at 28 °C for 48 h in darkness before colonies were counted.

180

181 *DNA extraction*

182

183 DNA extraction was performed in triplicates directly from the soil suspensions, following the protocol of
184 Lueders, Manefield & Friedrich. (2004) with slight modifications. Briefly, 600 µl of the soil suspensions
185 were mixed with 150 µl NaPO₄ buffer (600 mM), 250 µl TNS solution and 0.7 g of 0.1 mm silica beads.
186 Cells were lysed by beat-beating at 6.5 m s⁻¹ for 30 s. The subsequent extraction steps were done
187 according to the protocol. Finally, we eluted the DNA in 30 µl EB buffer. The quality of DNA extracts
188 were checked by electrophoresis on 1.5 % agarose gels at 120 V for 30 min. For all further analyses
189 triplicate samples were pooled.

190

191 *Quantitative real-time PCR*

192

193 We used quantitative real time PCR (qPCR) to enumerate total bacteria and specific disease-suppressive
194 bacteria, producing the antifungal metabolites 2,4-diacetylphloroglucinol (2,4-DAPG) and hydrogen
195 cyanide (HCN), which contribute to the suppression of fungal diseases in soil (Voisard *et al.* 1989; Weller
196 *at al.* 2002). All reactions were performed in a final reaction volume of 20 µl containing 2 µl of the
197 template DNA, 10 µl KAPA SYBR FAST qPCR MasterMix Universal (Kapa Biosystems, Wilmington,
198 MA, USA), 24 µg bovine serum albumin (BSA) and 0.24 µM of each of the respective primers. All
199 reactions were run in a Stratagene Mx3005P instrument (Agilent Technologies, Waldbronn, Germany). To
200 enumerate total bacteria, we quantified the copy numbers of 16s rDNA using the primer pair EUB338 and
201 EUB518 (Fierer *et al.* 2005). To enumerate HCN producing bacteria we quantified the copy numbers of
202 *hcnAB* using the primer pair PM2 and PM-26R (Svercel, Duffy & Défago 2007) and for 2,4-DAPG
203 producing bacteria we quantified the copy numbers of *phlD* using the primer pair BPF2 and BPR4
204 (McSpadden Gardener *et al.* 2001). As quantification standards we used a dilution series of already
205 quantified amplification products of the targeted fragments. For reactions targeting 16s and *hcnAB* the
206 standards were obtained from *P. protegens* strain CHA0 and for *phlD* from *P. fluorescens* strain Q2-87.
207 Additionally, we performed qPCR targeting *F. graminearum* DNA using the primer pair FG16NF and
208 FG16NR (Nicholson *et al.* 1998) to validate the success of pathogen inoculation and to check for potential
209 cross-contamination. Details of oligonucleotide primers and the cycling conditions are listed in
210 Supplementary Information Tables S1 and S2. Microcosms contaminated with *F. graminearum* (presence
211 of the fungus in one of the compartments of control plants or in the systemic compartment of the infected
212 plants respectively) were omitted from further analyses. This resulted in total of 10 replicated split-root
213 microcosms for the control treatment and 16 replicated microcosms for the infection treatment.

214

215 *Assessment of Pseudomonas community structure*

216

217 *Pseudomonas* community structure was investigated using an established denaturing gel gradient
218 electrophoresis (DGGE) based on a nested PCR amplification of the *Pseudomonas*-specific *gacA* gene
219 (Costa *et al.* 2007). We performed the first PCR using the primer pair *gacA*-1F (Costa *et al.* 2007) and
220 *gacA*2 (de Souza, Mazzola & Raaijmakers 2003). PCR was performed in a total reaction volume of 25 μ l
221 containing 1 μ l of the template DNA, 5 μ l KAPA2G Buffer A (Kapa Biosystems, Wilmington, MA,
222 USA), 1.25 U KAPA2G Robust DNA polymerase (Kapa Biosystems, Wilmington, MA, USA), 100 μ M
223 dNTPs and 0.2 μ M of each of the according primer. After purification, the products were subjected to a
224 second PCR using the primers *gacA*-1FGC and *gacA*-2R (Costa *et al.* 2007) in a final reaction volume of
225 25 μ l containing 1 μ l of the first PCR product as template, 5 μ l KAPA2G Buffer A, 1.25 U KAPA2G
226 Robust DNA polymerase, 100 μ M dNTPs and 0.2 μ M of each of the according primer. Both PCR were
227 performed in a TProfessional Thermal cycler (Analytik Jena, Jena, Germany). Details of oligonucleotide
228 primers and the cycling conditions are listed in the Supplementary Information (Table S1 and Table S2).
229 Electrophoresis was performed on 4 μ l of the second PCR product in an 8% acrylamide gel with a
230 denaturing gradient ranging from 20% to 80% denaturants (100% denaturants: 7M urea and 40%
231 formamide) at 60 °C for 18 h and 140 V in 1 x Tris-acetate-EDTA buffer using a Dcode Universal
232 Mutation Detection System (Bio-Rad, Hercules, CA, USA). The gels were stained with 200x SYBR
233 Green (Sigma-Aldrich, Hamburg, Germany). The DGGE fingerprints were digitized to greyscale images
234 and analyzed using the Quantity One software (Bio-Rad, Hercules, CA, USA).

235

236 *Bacterial chemotaxis towards infected and uninfected plants*

237

238 We assessed the chemotactic activity of a GFP-tagged *Pseudomonas protegens* CHA0 (Jousset *et al.*
239 2006) towards the exudates of infected and uninfected plants. We chose this strain as reference fluorescent
240 pseudomonad carrying the functional genes *phlD* and *hcnAB* also targeted in the natural soil experiment.
241 Bacteria were pre-grown in 3 g l⁻¹ tryptic soy broth (TSB) at 20 °C for 24 h, centrifuged (5 min at 10,000
242 rpm) and washed 5 times in 0.1 x PBS to remove remaining nutrients. Bacterial density was adjusted to

243 OD₆₀₀=0.1 in 0.1 x PBS. We used 200 µl pipette tips filled with 50 µl of the exudate samples, placed on a
244 multichannel pipette, as chemotaxis capillaries. The filled tips remained on the pipette and were carefully
245 placed into wells of a microtiter plate containing 100 µl of the bacterial suspension. The whole system was
246 incubated for 30 min at 20 °C in darkness to allow the bacteria migrating into the pipette tips. Bacterial
247 concentration in the pipette tips was measured by flow-cytometric enumeration using a BD Accuri C6
248 flow cytometer (Accuri, Ann Harbor, MI, USA) following the manufacturer's instructions. For both
249 treatments we set up 10 split-root microcosms as replicates.

250

251 *Statistical analyses*

252

253 All analyses were performed in R version 3.1.1 (R Core Team 2014). In the soil experiment, we tested for
254 the effect of the infection treatment on dry shoot biomass using a linear model (LM) with the infection
255 treatment (control vs. pathogen addition) as categorical predictor. To test for differences in root dry
256 biomass we used a linear model with the infection treatment, the compartment side (treatment
257 compartment vs. systemic compartment) and their interaction as categorical predictors.

258 In the soil experiment, bacterial and gene abundances were calculated as numbers of gene copies and
259 colony forming units (CFU) per gram soil dry weight respectively. We calculated *gacA* allelic richness as
260 the number of bands within each gel lane.

261 Because soil water is essential for bacterial motility, we included the soil water content (percentage soil
262 moisture) as covariate in the models targeting bacterial abundances, gene abundances and *gacA* allelic
263 richness in the soil experiment. The soil water content was not affected by the infection treatment
264 ($F_{1,48}=0.51$, $p=0.48$), the compartment side ($F_{1,48}=0.06$, $p=0.81$) nor their interaction ($F_{1,48}=0.60$, $p=0.44$),
265 indicating that there was no systematic bias.

266 Bacterial and gene abundances in the soil experiment exhibited a positive, right-skewed distribution with
267 an over proportional increase in variance. Thus, we used generalized linear models (GLM) with gamma
268 distributed errors and a log-link function (Faraway 2006; Crawley 2007), testing for the effects of the soil

269 water content (linear covariate), the infection treatment (factor with two levels), the compartment side
270 (factor with two levels) and the treatment-compartment side interaction as categorical predictors.

271 Regarding the analysis of *gacA* allelic richness in the soil experiment, it is noteworthy, that the treatments
272 were represented in equal proportions within a single gel, while the compartment sides were represented
273 on separate gels. Therefore, we tested for the effect of the infection treatment on *gacA* allelic richness
274 separately for the compartment sides using linear models and fitted the gel identity as a block effect before
275 the soil water content and infection treatment. To adjust for the covariate soil water content, we calculated
276 for all above mentioned response variables their least-square means and standard errors (r-package:
277 lsmeans; Lenth 2015) based on the respective model (GLMs targeting bacterial and gene abundances and
278 LMs targeting *gacA* allelic richness).

279 For the chemotaxis experiment, we defined chemo-attractant function of root exudates as the density of *P.*
280 *protegens* CHA0 (cells μl^{-1} exudate) in capillaries filled with the root exudates. We tested for effects of
281 the infection treatment, the compartment side and their interaction as categorical predictors on the chemo-
282 attractant function of root exudates using a GLM with gamma distributed errors and a log-link function. If
283 the models indicated differing effects of the infection treatment between the compartment sides (infection
284 treatment x compartment side interaction at $p < 0.1$), we additionally tested the pairwise contrasts of the
285 infection treatments within both compartments sides (r-package: multcomp; Hothorn, Bretz & Westfall
286 2008).

287 The *gacA* community composition was analyzed using non-metric multidimensional scaling (NMDS)
288 based on pairwise Bray-Curtis dissimilarities of the Hellinger-transformed (Legendre & Legendre 1998;
289 Legendre & Gallagher 2001; Ramette 2007) greyscale band intensities. First, ordination was performed
290 separately for each single gel to account for inter-gel variations resulting from potential differences of the
291 denaturing gradient due to the gel casting procedure. To check for the comparability of the ordination
292 results, we tested for the concordance of the single-gel ordinations within each compartment side using a
293 procrustes rotation test based on 999 permutations. Within the compartment sides we tested for the
294 significance of the infection treatment on the grouping of the *gacA* ordinations using permutational

295 multivariate analysis of variance (PERMANOVA) based on 999 permutations. Therefore, we constrained
296 the permutations within the single gels to account for gel identity in sense of a statistical block effect (r-
297 package: vegan; Oksanen *et al.* 2013).

298

299 **Results**

300

301 Dry shoot biomass of barley plants was not affected by the infection treatment ($F_{1,24}=0.01$, $p=0.91$). Also
302 dry root biomass was not affected by infection treatment ($F_{1,48}=0.43$, $p=0.51$), the compartment side
303 ($F_{1,48}=1.78$, $p=0.19$) nor their interaction ($F_{1,48}=0.04$, $p=0.84$), indicating that *F. graminearum* did not
304 generate measurable damage during the short incubation time.

305 The abundance of total heterotrophic bacteria (CFU on R2A medium) was not affected by any predictor
306 (Table 1, Fig. 1a). In contrast, the abundance of fluorescent pseudomonads (CFU on Gould's S1 medium)
307 was higher in the rhizosphere of infected plants than of uninfected plants at the systemic compartment
308 (Table 1, Fig. 1b). Further, the abundance of fluorescent pseudomonads was positively correlated with the
309 soil water content (Table 1, Fig. 2a).

310 Similar to the abundance of total heterotrophic bacteria, there were no effects of any predictor on the
311 abundance of 16s rDNA gene copy numbers (Table 1, Fig. 3a). However, the abundances of the two
312 assessed antifungal genes (*phlD* and *hcnAB*) were positively correlated with the soil water content (Table
313 1, Fig. 2b,c). The effect of the infection treatment on antifungal gene abundance depended on the
314 compartment side (Table 1) and their abundances were higher in the rhizosphere of infected plants than of
315 uninfected plants at the systemic compartments (Fig. 3a,b). In the treatment compartment, *gacA* allelic
316 richness was not significantly affected by the infection treatment (Table 2). However, in the systemic
317 compartment, *gacA* allelic richness was higher in the rhizosphere of infected plants than of uninfected
318 plants (Table 2, Fig. 4a).

319 Procrustes rotation test revealed that the single gel ordinations of the *gacA* DGGE profiles were congruent
320 in the systemic compartments ($p=0.017$), indicating a coherent structuring force on the communities.

321 Further, community composition was well discriminated by the infection treatment in the systemic
322 compartment (Table 2, Fig. 4b). The single gel ordinations in the treatment compartment were not
323 congruent ($p=0.15$) and community composition was not separated regarding the infection treatment
324 (Table 2, Fig. 4b).

325 In the chemotaxis experiment, *P. protegens* CHA0 was more attracted by the root exudates of infected
326 plants than by the root exudates of the control plants. This increase was independent of the compartment
327 side (Table 1, Fig 5).

328

329 **Discussion**

330

331 The results of our study show an enrichment of the rhizosphere microbiome with potentially antifungal
332 microbes for barley plants challenged with *F. graminearum*. By combining a split-root approach with
333 different levels of resolution (zooming from all bacteria into one representative taxonomic group and two
334 representative functional genes), we could disentangle the effects of plant mediated microbiome
335 structuring from perturbations of the infection treatment.

336 Our results provide evidence for the concept that plants are able to actively recruit specific bacterial
337 groups upon pathogen infection. Fluorescent pseudomonad abundance increased with infection. These
338 bacteria are good colonizers of plant roots (Loper *et al.* 2012) and we propose that their enrichment in the
339 rhizosphere of infected plants may be explained by conserved characteristics such as chemotactic activity
340 toward root exudates. The fact that fluorescent pseudomonads are repeatedly associated with disease
341 suppression (Weller 2007; Mendes *et al.* 2011) makes it plausible that a co-evolutionary process between
342 plants and this bacterial group occurred, in which bacteria evolved to respond to plant alarm cues.

343 However, we can only speculate about the underlying mechanism. In contrast to symbioses with rhizobia
344 or mycorrhiza, plants have very few possibilities to select for partners providing a particular function such
345 as disease protection (Kiers & Denison 2008). We propose that feedback loops, such as the enhanced

346 exudation in presence of 2,4-DAPG (Philips *et al.* 2004), may provide a reward mechanism that may have
347 promoted the recruitment of bacteria harboring antifungal traits.

348 Bacterial recruitment can be the result of a specific attraction by exudates or by a higher growth on roots.
349 Chemotaxis appears here as a significant driver. Exudates from infected plants were more attractive than
350 exudates of uninfected plants for *P. protegens* CHA0, a model strain harboring the genes needed for the
351 production of both 2,4-DAPG and HCN, the two genes that were systemically enriched in the rhizosphere
352 of infected plants. These results are in line with a past study on *Bacillus*, showing that plants challenged
353 by the foliar pathogen *Pseudomonas syringae* recruited one specific *Bacillus* strain by secreting more
354 malic acid, to which the studied *Bacillus* strain showed a strong chemotactic response (Rudrappa *et al.*
355 2008). We propose that a similar effect occurred in the soil experiment with fluorescent pseudomonads.
356 The chemotaxis hypothesis is further backed by the importance of the soil water content for bacterial
357 recruitment. High soil moisture promotes the motility of free living bacteria (Wong & Griffin 1976) as
358 well as the diffusion of soluble nutrients and chemo-attractant compounds in the soil matrix (Raynaud
359 2010). The positive effect of the soil water content on the abundance of fluorescent pseudomonads and
360 antifungal genes indicates that the recruitment process is driven by increased migration of motile bacteria
361 towards the rhizosphere of the plants. Fluorescent pseudomonads are highly motile bacteria, which is an
362 important trait related to their rhizosphere competence (Turnbull *et al.* 2001; de Weert *et al.* 2002;
363 Martínez-Granero, Rivilla & Martín 2006). The hypothesis of plant triggered migration of disease-
364 suppressive bacteria is also supported by the chemotaxis experiment, documenting that sterile root
365 exudates from infected plants were more attractive to *P. protegens* than those from control plants. Root
366 exudates serve the plant to communicate with surrounding microbes and their composition can shift in
367 presence of pathogens. For instance, organic acids exert an attracting cue for the chemotactic activity of
368 fluorescent pseudomonads (Oku *et al.* 2014). Plants can rapidly change their exudation profile in response
369 to pathogen infection and initiate the synthesis of defensive organic acids to suppress pathogens (Lanoue
370 *et al.* 2010). Some of these compounds also stimulate the expression of antifungal genes (Jousset *et al.*
371 2011).

372 Alternatively, an increased water potential can rapidly lead to an increased bacterial biomass (Lund &
373 Goksøyr 1980; Kieft, Soroker & Firestone 1987). In both scenarios we propose that sufficiently high soil
374 moisture is essential for the plant to recruit beneficial microbes out of the existing microbial species pool.
375 Pseudomonad richness, measured as *gacA* allelic richness, was higher in the rhizosphere of infected plants
376 than of uninfected plants. This fits with an enhanced chemo-attractant function of the root exudates of
377 infected plants. For instance, infected plants may have recruited bacteria from more distant soil regions,
378 which would allow accessing a broader microbial species pool. This higher diversity may be crucial for
379 efficient disease suppression as it may enhance the production of antifungal metabolites (Jousset *et al.*
380 2014). The distinctiveness of the bacterial community compositions between the rhizosphere of infected
381 plants and uninfected plants at the systemic compartments further suggests that this selective plant driven
382 recruitment functions as a structuring force for the assembly of rhizosphere bacteria.

383

384 *Caveats*

385

386 We observed enrichments of specific bacteria due to the infection treatment in the systemic compartment
387 only. This leads us to propose that the inoculum application may locally interfere with plant driven effects
388 as observed at the systemic compartments. The addition of PBS to the treatment compartment may have
389 affected microbial communities via an addition of phosphorus or a mechanical perturbation of the root
390 system. Even if we kept perturbation as low as possible by using highly diluted PBS and dripping it slowly
391 onto the roots, it may account for some effects such as the higher bacterial abundances in the treatment
392 compartment than the systemic compartment. Also effects of the fungal inoculum itself, e.g. an
393 antagonistic (Notz *et al.* 2002) or attracting potential of fungal metabolites (de Weert *et al.* 2004), may
394 mask plant driven processes. Such concomitant effects illustrate how important it is to physically separate
395 the site of experimental manipulation from the site of measurements especially in the context of systemic
396 plant driven processes.

397 This study focused on one specific plant-pathogen system and on three very simplified bacterial groups
398 (all bacteria, one specific taxon and two functional genes). Also the plants were grown for a short time in
399 small microcosms under the controlled conditions of a climate chamber. The potential differences to other
400 plant-pathogen systems and the impact of environmental conditions or plant age remains a subject for
401 further investigation, which would give valuable insights into the generality and limitations of the process
402 observed in this study. Nevertheless, this simplification allowed us to conceptually demonstrate a new
403 dimension in plant-microbiome interactions, disentangling effects of a host plant and a pathogen on the
404 composition and functionality of microbial communities. However, this approach also brings a few
405 caveats we would like to address. First, we would like to emphasize that the tested groups are examples.
406 Microbial communities are very diverse, both phylogenetically and functionally. Further, we did not
407 attempt to analyze exudate composition, as they would have in the present context added few to the
408 observed net effects on bacteria. Rather, we see our approach as a conceptual base that can be combined
409 with metabolomics or metagenomics to disentangle the roles of plant and pathogen on the assembly of the
410 rhizosphere microbiome. Further, we did not assess the antifungal potential of root-associated bacteria.
411 We propose that future studies assessing soil suppressiveness in the systemic compartment after several
412 growth cycles may greatly improve our understanding of the role of the plants in building up soil
413 suppressiveness as observed in take-all decline (Weller *et al.* 2002).

414

415 **Conclusion**

416

417 We demonstrated that barley plants actively manipulate their rhizosphere community to favor a specific
418 function, such as here antifungal traits, in response to pathogen attack. This extends the finding from
419 Jousset *et al.* (2011) showing a stimulation of antifungal gene expression in bacteria living on pathogen
420 infested plants to the recruitment and enrichment of disease-suppressive bacteria in a non-sterile soil
421 system. The specificity of the recruitment indicates an active selection process by the plant and its
422 restriction to non-infected parts of the root systems suggests that pathogen presence or infection-linked

423 damages to the plant may reduce the ability of plants to select for beneficial microbes. The identification
424 of the ability of plants to recruit beneficial microbes to counteract pathogens remains a challenge for plant
425 breeding (Haney *et al.* 2015). Our study provides a new strategy to assess a plant`s potential to recruit
426 disease-suppressive bacteria by removing the noise caused by pathogen infection.

427

428 **Acknowledgements**

429

430 We thank Petr Karlovsky (Department of Molecular Phytopathology and Mycotoxin Research, University
431 of Göttingen, Germany) for providing the fungal cultures and the primers used for fungal detection in the
432 soil experiment.

433

434 **Data accessibility**

435

436 Data associated with this study are deposited in the Dryad repository: doi:10.5061/dryad.83np7.

437

438 **References**

- 439 Aira, M., Gómez-Brandón, M., Lazcano, C., Bååth, E. & Domínguez, J. (2010) Plant genotype strongly
440 modifies the structure and growth of maize rhizosphere microbial communities. *Soil Biology and*
441 *Biochemistry*, **42**, 2276–2281.
- 442 Bais, H.P., Weir, T.L., Perry, L.G., Gilroy, S. & Vivanco, J.M. (2006) The role of root exudates in
443 rhizosphere interactions with plants and other organisms. *Annual Review of Plant Biology*, **57**, 233–266.
- 444 Bakker, P.A., Doornbos, R.F., Zamioudis, C., Berendsen, R.L. & Pieterse, C.M. (2013) Induced systemic
445 resistance and the rhizosphere microbiome. *The Plant Pathology Journal*, **29**, 136–143.
- 446 Berendsen, R.L., Pieterse, C.M. & Bakker, P.A. (2012) The rhizosphere microbiome and plant health.
447 *Trends in Plant Science*, **17**, 478–486.
- 448 Bulgarelli, D., Garrido-Oter, R., Münch, P.C., Weiman, A., Dröge, J., Pan, Y., McHardy, A.C. & Schulze-
449 Lefert, P. (2015) Structure and function of the bacterial root microbiota in wild and domesticated barley.
450 *Cell Host & Microbe*, **17**, 392–403.
- 451 Chaparro, J.M., Badri, D.V., Bakker, M.G., Sugiyama, A., Manter, D.K. & Vivanco, J.M. (2013) Root
452 exudation of phytochemicals in Arabidopsis follows specific patterns that are developmentally
453 programmed and correlate with soil microbial functions. *PloS one*, **8**, e55731.
- 454 Costa, R.G., Götz, M., Mrotzek, N., Lottmann, J., Berg, G. & Smalla, K. (2006) Effects of site and plant
455 species on rhizosphere community structure as revealed by molecular analysis of microbial guilds. *FEMS*
456 *Microbiology Ecology*, **56**, 236–249.
- 457 Costa, R.G., Newton, C.M., Kroegerrecklenfort, E., Opelt, K., Berg, G. & Smalla, K. (2007)
458 *Pseudomonas* community structure and antagonistic potential in the rhizosphere: insights gained by
459 combining phylogenetic and functional gene-based analyses. *Environmental Microbiology*, **9**, 2260–2273.
- 460 Crawley, M.J. (2007) *The R book*. Wiley, Chichester.

461 De Souza, J.T., Mazzola, M. & Raaijmakers, J.M. (2003) Conservation of the response regulator gene
462 *gacA* in *Pseudomonas* species. *Environmental Microbiology*, **5**, 1328–1340.

463 De Weert, S., Vermeiren, H., Mulders, I.H., Kuiper, I., Hendrickx, N., Bloemberg, G.V., Vanderleyden, J.,
464 de Mot, R. & Lugtenberg, B.J. (2002) Flagella-driven chemotaxis towards exudate components is an
465 important trait for tomato root colonization by *Pseudomonas fluorescens*. *Molecular Plant-Microbe*
466 *Interactions*, **15**, 1173–1180.

467 De Weert, S., Kuiper, I., Lagendijk, E.L., Lamers, G.E. & Lugtenberg, B.J. (2004) Role of chemotaxis
468 toward fusaric acid in colonization of hyphae of *Fusarium oxysporum* f. sp. *radicis-lycopersici* by
469 *Pseudomonas fluorescens* WCS365. *Molecular Plant-Microbe Interactions*, **17**, 1185–1191.

470 D’Mello, J., Placinta, C.M. & Macdonald, A. (1999) Fusarium mycotoxins: a review of global
471 implications for animal health, welfare and productivity. *Animal Feed Science and Technology*, **80**, 183–
472 205.

473 Faraway, J.J. (2006) *Extending the linear model with R. Generalized linear, mixed effects and*
474 *nonparametric regression models*. Chapman & Hall/CRC, Boca Raton.

475 Fierer, N., Jackson, J.A., Vilgalys, R. & Jackson, R.B. (2005) Assessment of soil microbial community
476 structure by use of taxon-specific quantitative PCR assays. *Applied and Environmental Microbiology*, **71**,
477 4117–4120.

478 Goswami, R.S. & Kistler, H.C. (2004) Heading for disaster: *Fusarium graminearum* on cereal crops.
479 *Molecular Plant Pathology*, **5**, 515–525.

480 Gould, W.D., Hagedorn, C., Bardinelli, T.R. & Zablutowicz, R.M. (1985) New selective media for
481 enumeration and recovery of fluorescent pseudomonads from various habitats. *Applied and Environmental*
482 *Microbiology*, **49**, 28–32.

483 Haney, C.H., Samuel, B.S., Bush, J. & Ausubel, F.M. (2015) Associations with rhizosphere bacteria can
484 confer an adaptive advantage to plants. *Nature Plants*, **1**, 15051.

485 Henkes, G.J., Jousset, A., Bonkowski, M., Thorpe, M.R., Scheu, S., Lanoue, A., Schurr, U. & Röse, U.S.
486 (2010) *Pseudomonas fluorescens* CHA0 maintains carbon delivery to *Fusarium graminearum*-infected
487 roots and prevents reduction in biomass of barley shoots through systemic interactions. *Journal of*
488 *Experimental Botany*, **62**, 4337–4344.

489 Hothorn, T., Bretz, F. & Westfall, P. (2008) Simultaneous inference in general parametric models.
490 *Biometrical Journal*, **50**, 346–363.

491 Jousset, A., Lara, E., Wall, L.G. & Valverde, C. (2006) Secondary metabolites help biocontrol strain
492 *Pseudomonas fluorescens* CHA0 to escape protozoan grazing. *Applied and Environmental Microbiology*,
493 **72**, 7083–7090.

494 Jousset, A., Rochat, L., Lanoue, A., Bonkowski, M., Keel, C. & Scheu, S. (2011) Plants respond to
495 pathogen infection by enhancing the antifungal gene expression of root-associated bacteria. *Molecular*
496 *Plant-Microbe Interactions*, **24**, 352–358.

497 Jousset, A., Becker, J., Chatterjee, S., Karlovsky, P., Scheu, S. & Eisenhauer, N. (2014) Biodiversity and
498 species identity shape the antifungal activity of bacterial communities. *Ecology*, **95**, 1184–1190.

499 Kazan, K., Gardiner, D.M. & Manners, J.M. (2012) On the trail of a cereal killer: recent advances in
500 *Fusarium graminearum* pathogenomics and host resistance. *Molecular Plant Pathology*, **13**, 399–413.

501 Kieft, T.L., Soroker, E. & Firestone, M.K. (1987) Microbial biomass response to a rapid increase in water
502 potential when dry soil is wetted. *Soil Biology and Biochemistry*, **19**, 119–126.

503 Kiers, E.T. & Denison, R.F. (2008) Sanctions, cooperation, and the stability of plant-rhizosphere
504 mutualisms. *Annual Review of Ecology, Evolution, and Systematics*, **39**, 215–236.

505 Klironomos, J.N. (2002) Feedback with soil biota contributes to plant rarity and invasiveness in
506 communities. *Nature*, **417**, 67–70.

507 Lanoue, A., Burlat, V., Henkes, G.J., Koch, I., Schurr, U. & Röse, U.S. (2010). De novo biosynthesis of
508 defense root exudates in response to *Fusarium* attack in barley. *New Phytologist*, **185**, 577–588.

509 Legendre, P. & Gallagher, E. (2001) Ecologically meaningful transformations for ordination of species
510 data. *Oecologia*, **129**, 271–280.

511 Legendre, P. & Legendre, L. (1998) *Numerical ecology*. Elsevier, Amsterdam.

512 Lenth, R.V. (2015) *lsmeans: Least-Squares Means*. R-package version 2.20-2. [http://CRAN.R-](http://CRAN.R-project.org/package=lsmeans)
513 [project.org/package=lsmeans](http://CRAN.R-project.org/package=lsmeans)

514 Loper, J.E., Hassan, K.A., Mavrodi, D.V., Davis, E.W., Lim, C.K., Shaffer, B.T., Elbourne, Liam D H,
515 Stockwell, V.O., Hartney, S.L., Breakwell, K., Henkels, M.D., Tetu, S.G., Rangel, L.I., Kidarsa, T.A.,
516 Wilson, N.L., van de Mortel, Judith E, Song, C., Blumhagen, R., Radune, D., Hostetler, J.B., Brinkac,
517 L.M., Durkin, A.S., Kluepfel, D.A., Wechter, W.P., Anderson, A.J., Kim, Y.C., Pierson, L.S., Pierson,
518 E.A., Lindow, S.E., Kobayashi, D.Y., Raaijmakers, J.M., Weller, D.M., Thomashow, L.S., Allen, A.E. &
519 Paulsen, I.T. (2012) Comparative genomics of plant-associated *Pseudomonas* spp.: insights into diversity
520 and inheritance of traits involved in multitrophic interactions. *PLoS genetics*, **8**, e1002784.

521 Lueders, T., Manefield, M. & Friedrich, M.W. (2004) Enhanced sensitivity of DNA- and rRNA-based
522 stable isotope probing by fractionation and quantitative analysis of isopycnic centrifugation gradients.
523 *Environmental Microbiology*, **6**, 73–78.

524 Lund, V. & Goksøyr, J. (1980) Effects of water fluctuations on microbial mass and activity in soil.
525 *Microbial Ecology*, **6**, 115–123.

526 Martínez-Granero, F., Rivilla, R. & Martín, M. (2006) Rhizosphere selection of highly motile phenotypic
527 variants of *Pseudomonas fluorescens* with enhanced competitive colonization ability. *Applied and*
528 *Environmental Microbiology*, **72**, 3429–3434.

529 McSpadden Gardener, B.B., Mavrodi, D.V., Thomashow, L.S. & Weller, D.M. (2001) A rapid polymerase
530 chain reaction-based assay characterizing rhizosphere populations of 2,4-diacetylphloroglucinol-
531 producing bacteria. *Phytopathology*, **91**, 44–54.

532 Mendes, R., Kruijt, M., de Bruijn, I., Dekkers, E., van der Voort, M., Schneider, J.H., Piceno, Y.M.,
533 DeSantis, T.Z., Andersen, G.L., Bakker, P.A. & Raaijmakers, J.M. (2011) Deciphering the rhizosphere
534 microbiome for disease-suppressive bacteria. *Science*, **332**, 1097–1100.

535 Müller, M.S., Scheu, S. & Jousset, A. (2013) Protozoa drive the dynamics of culturable biocontrol
536 bacterial communities. *PloS one*, **8**, e66200.

537 Newton, A.C., Flavell, A.J., George, T.S., Leat, P., Mullholland, B., Ramsay, L., Revoredo-Giha, C.,
538 Russell, J., Steffenson, B.J., Swanston, J.S., Thomas, W.T.B., Waugh, R., White, P.J. & Bingham, I.J.
539 (2011) Crops that feed the world 4. Barley: a resilient crop? Strengths and weaknesses in the context of
540 food security. *Food Security*, **3**, 141–178.

541 Nicholson, P., Simpson, D., Weston, G., Rezanoor, H., Lees, A., Parry, D. & Joyce, D. (1998) Detection
542 and quantification of *Fusarium culmorum* and *Fusarium graminearum* in cereals using PCR assays.
543 *Physiological and Molecular Plant Pathology*, **53**, 17–37.

544 Notz, R., Maurhofer, M., Dubach, H., Haas, D. & Defago, G. (2002) Fusaric acid-producing strains of
545 *Fusarium oxysporum* alter 2,4-Diacetylphloroglucinol biosynthetic gene expression in *Pseudomonas*
546 *fluorescens* CHA0 in vitro and in the rhizosphere of wheat. *Applied and Environmental Microbiology*, **68**,
547 2229–2235.

548 Oksanen, J., Blanchet, G.F., Kindt, R., Legendre, P., Minchin, P.R., O'Hara, R.B., Simpson, G.L.,
549 Solymos, P., Stevens, M.H. & Wagner, H. (2013) *vegan: Community Ecology Package*. R-package
550 version 2.0-10. <http://CRAN.R-project.org/package=vegan>

551 Oku, S., Komatsu, A., Nakashimada, Y., Tajima, T. & Kato, J. (2014) Identification of *Pseudomonas*
552 *fluorescens* chemotaxis sensory proteins for malate, succinate, and fumarate, and their involvement in root
553 colonization. *Microbes and Environments*, **29**, 413–419.

554 Packer, A. & Clay, K. (2000) Soil pathogens and spatial patterns of seedling mortality in a temperate tree.
555 *Nature*, **404**, 278–281.

556 Peiffer, J.A., Spor, A., Koren, O., Jin, Z., Tringe, S.G., Dangl, J.L., Buckler, E.S. & Ley, R.E. (2013)
557 Diversity and heritability of the maize rhizosphere microbiome under field conditions. *Proceedings of the*
558 *National Academy of Sciences of the United States of America*, **110**, 6548–6553.

559 Petermann, J.S., Fergus, A.J.F., Turnbull, L.A. & Schmid, B. (2008) Janzen-Connell effects are
560 widespread and strong enough to maintain diversity in grasslands. *Ecology*, **89**, 2399–2406.

561 Phillips, D.A., Fox, T.C., King, M.D., Bhuvaneswari, T.V. & Teuber, L.R. (2004) Microbial products
562 trigger amino acid exudation from plant roots. *Plant Physiology*, **136**, 2887–2894.

563 R Core Team (2014) R: A language and environment for statistical computing. R Foundation for
564 Statistical Computing, Vienna, Austria. <http://www.R-project.org>.

565 Ramette, A. (2007) Multivariate analyses in microbial ecology. *FEMS Microbiology Ecology*, **62**, 142–
566 160.

567 Raynaud, X. (2010) Soil properties are key determinants for the development of exudate gradients in a
568 rhizosphere simulation model. *Soil Biology and Biochemistry*, **42**, 210–219.

569 Reasoner, D.J. & Geldreich, E.E. (1985) A new medium for the enumeration and subculture of bacteria
570 from potable water. *Applied and Environmental Microbiology*, **49**, 1–7.

571 Rudrappa, T., Czymmek, K.J., Paré, P.W. & Bais, H.P. (2008) Root-secreted malic acid recruits beneficial
572 soil bacteria. *Plant Physiology*, **148**, 1547–1556.

573 Strange, R.N. & Scott, P.R. (2005) Plant disease: a threat to global food security. *Annual Review of*
574 *Phytopathology*, **43**, 83–116.

575 Svercel, M., Duffy, B. & Défago, G. (2007) PCR amplification of hydrogen cyanide biosynthetic locus
576 *hcnAB* in *Pseudomonas* spp. *Journal of Microbiological Methods*, **70**, 209–213.

577 Trivedi, P., He, Z., Van Nostrand, Joy D, Albrigo, G., Zhou, J. & Wang, N. (2012) Huanglongbing alters
578 the structure and functional diversity of microbial communities associated with citrus rhizosphere. *The*
579 *ISME Journal*, **6**, 363–383.

580 Turnbull, G.A., Morgan, J.W., Whipps, J.M. & Saunders, J.R. (2001) The role of bacterial motility in the
581 survival and spread of *Pseudomonas fluorescens* in soil and in the attachment and colonisation of wheat
582 roots. *FEMS Microbiology Ecology*, **36**, 21–31.

583 Van der Putten, W.H. (2003) Plant defense belowground and spatiotemporal processes in natural
584 vegetation. *Ecology*, **84**, 2269–2280.

585 Voisard, C., Keel, C., Haas, H. & Défago, G. (1989) Cyanide production by *Pseudomonas fluorescens*
586 helps suppress black root rot of tobacco under gnotobiotic conditions. *EMBO Journal*, **8**, 351–358.

587 Weller, D.M., Raaijmakers, J.M., Gardener, B.B. & Thomashow, L.S. (2002) Microbial populations
588 responsible for specific soil suppressiveness to plant pathogens. *Annual Review of Phytopathology*, **40**,
589 309–348.

590 Weller, D.M. (2007) *Pseudomonas* biocontrol agents of soilborne pathogens: looking back over 30 years.
591 *Phytopathology*, **97**, 250–256.

592 Wong, P. & Griffin, D.M. (1976) Bacterial movement at high matric potentials—I. In artificial and natural
593 soils. *Soil Biology and Biochemistry*, **8**, 215–218.

594 Yuan, J., Chaparro, J.M., Manter, D.K., Zhang, R., Vivanco, J.M. & Shen, Q. (2015) Roots from distinct
595 plant developmental stages are capable of rapidly selecting their own microbiome without the influence of
596 environmental and soil edaphic factors. *Soil Biology and Biochemistry*, **89**, 206–209.

597

598 **Table 1** Results of the generalized linear models (with gamma distributed errors and a log-link function)
 599 targeting the abundances of total heterotrophic bacteria (CFU on R2A medium), fluorescent
 600 pseudomonads (CFU on Gould's S1 medium), 16s rDNA, the antifungal genes *hcnAB* and *phlD* in the
 601 rhizosphere of barley plants (soil experiment) and the chemo-attractant function of root exudates
 602 (chemotaxis experiment). In all models of the soil experiment the soil water content was fitted as linear
 603 covariate before the fixed effects of the infection treatment and the compartment side. Significant effects
 604 are highlighted in bold.

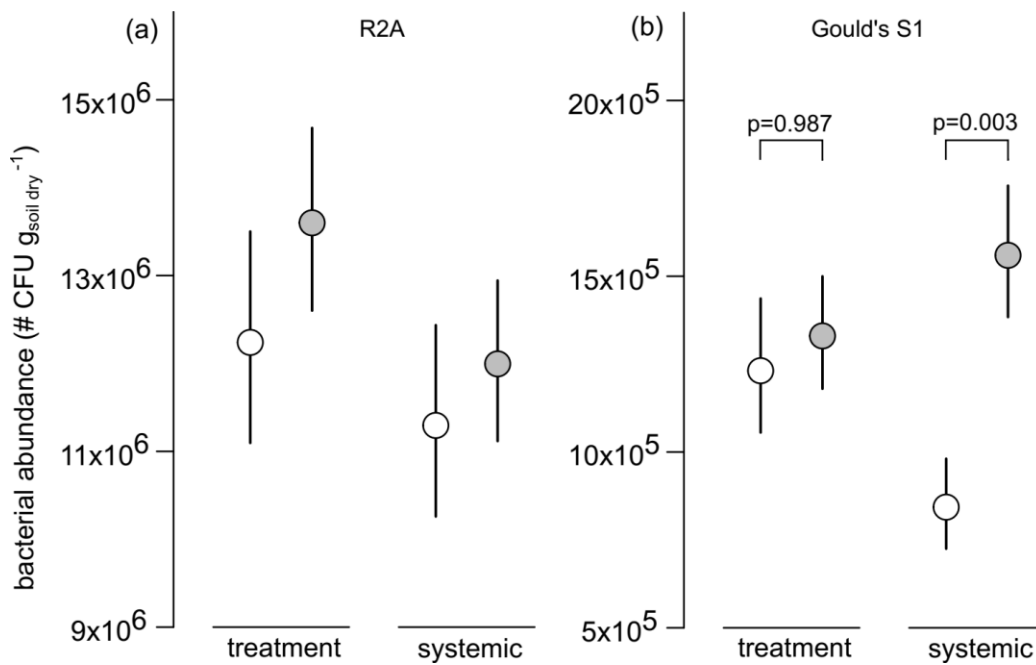
605	Response	Predictor	DF	Deviance	F	P
606	Total heterotrophic bacteria (# CFU g _{soil dry} ⁻¹)	Soil water content	1	0.049	0.538	0.467
607		Infection treatment (IT)	1	0.086	0.937	0.338
608		Compartment side (CS)	1	0.156	1.698	0.199
609		IT x CS	1	0.007	0.072	0.790
610		Residuals	47	4.202		
611	Fluorescent pseudomonads (# CFU g _{soil dry} ⁻¹)	Soil water content	1	5.970	26.818	<0.001
612		Infection treatment (IT)	1	1.455	6.538	<0.05
613		Compartment side (CS)	1	0.002	0.010	0.920
614		IT x CS	1	0.722	3.243	0.078
615		Residuals	47	10.226		
616	16s (# copies g _{soil dry} ⁻¹)	Soil water content	1	0.180	3.389	0.072
617		Infection treatment (IT)	1	0.104	1.969	0.167
618		Compartment side (CS)	1	0.001	0.017	0.897
619		IT x CS	1	0.002	0.044	0.836
620		Residuals	47	2.471		
621	<i>phlD</i> (# copies g _{soil dry} ⁻¹)	Soil water content	1	9.503	14.205	<0.001
622		Infection treatment	1	0.891	1.332	0.254
623		Compartment side	1	0.949	1.418	0.240
624		IT x CS	1	3.459	5.171	<0.05
625		Residuals	47	32.337		
626	<i>hcnAB</i> (# copies g _{soil dry} ⁻¹)	Soil water content	1	6.264	18.002	<0.001
627		Infection treatment (IT)	1	0.273	0.783	0.381
628		Compartment side (CS)	1	0.073	0.210	0.649
629		IT x CS	1	2.522	7.247	<0.01
630		Residuals	47	18.352		
631	Chemo-attractant function (cells μl ⁻¹ exudate)	Infection treatment (IT)	1	1.529	4.457	<0.05
632		Compartment side (CS)	1	0.260	0.759	0.389
633		IT x CS	1	0.109	0.317	0.577
634		Residuals	36	12.350		

635

636 **Table 2** Results of the linear models (LM) targeting *gacA* allelic richness and the permutational
637 multivariate analysis of variance (PERMANOVA) targeting the differences in the *gacA* community
638 compositions. All analyses were performed separately for each compartment side. The gel identity was
639 fitted before the soil water content and the infection treatment in the LMs. Permutations in the
640 PERMANOVAs were constrained within the single gels.

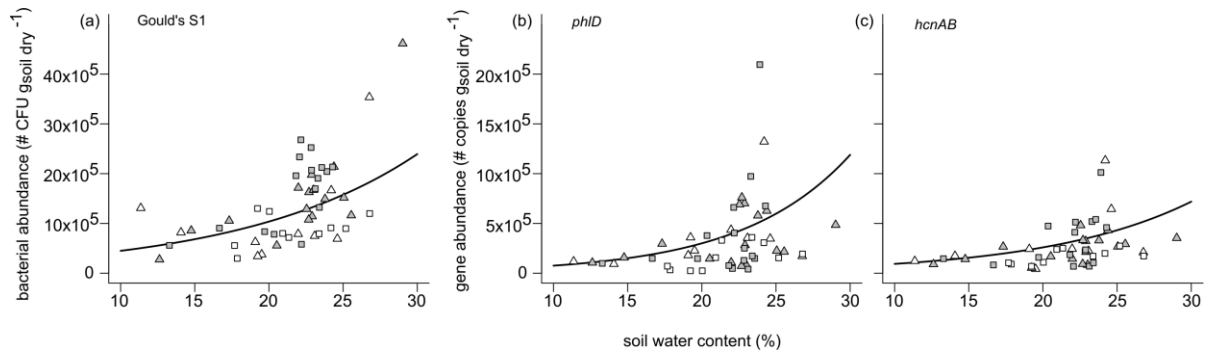
641	Response	Compartment side	Predictor	DF	SS	F	P
642			Gel identity	1	30.154	4.560	<0.05
643		Treatment	Soil water content	1	0.529	0.080	0.778
644			Infection treatment	1	4.307	0.651	0.428
645	<i>gacA</i> richness		Residuals	22	145.472		
646	(# bands)		Gel identity	1	5.538	2.632	0.119
647		Systemic	Soil water content	1	6.135	2.916	0.102
648			Infection treatment	1	42.034	19.976	<0.001
649			Residuals	22	46.293		
650		Treatment	Infection treatment	1	0.023	0.377	0.767
651	<i>gacA</i> composition		Residuals	24	1.472		
652	(NMDS)	Systemic	Infection treatment	1	0.185	2.018	<0.001
653			Residuals	24	2.197		
654							

655 **Fig 1** Abundance (least-square means and standard errors) of (a) total heterotrophic bacteria (CFU on R2A
 656 medium) and (b) fluorescent pseudomonads (CFU on Gould's S1 medium) in the rhizosphere of
 657 uninfected plants (white circles, left) and infected plants (grey circles, right) of the soil experiment.
 658 Treatment compartments are paired to the left and the systemic compartments are paired to the right. For
 659 significant infection treatment x compartment side interactions ($p < 0.1$) additional p-values are given for
 660 the pairwise contrasts of the infection treatment within each compartment side.



661

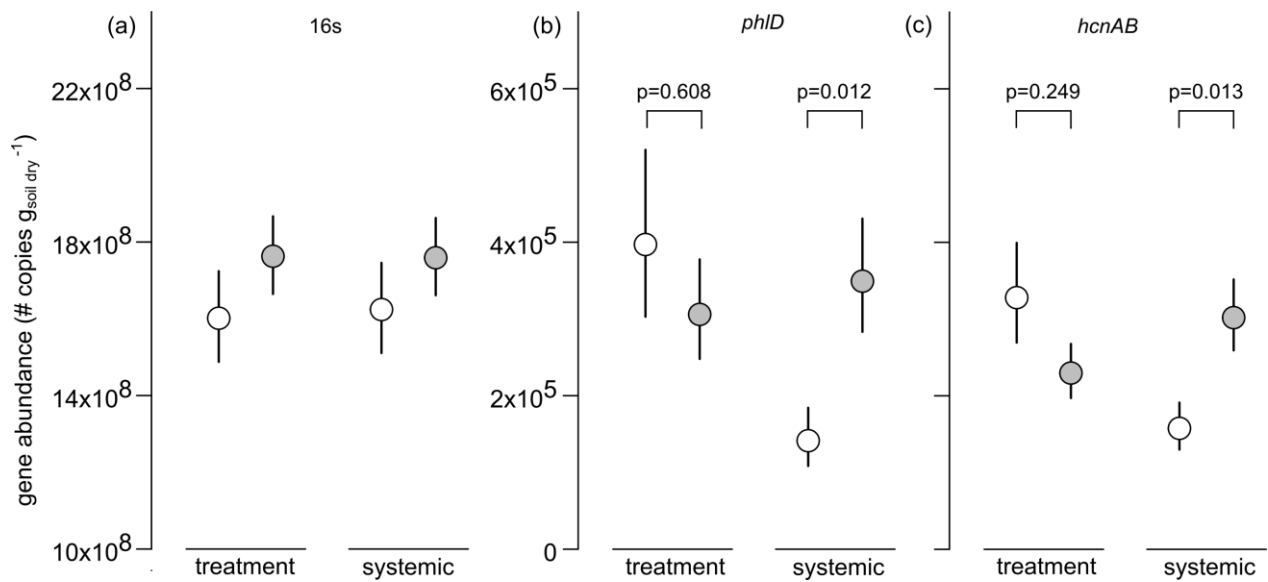
662 **Fig 2** Effect of the soil water content on the abundances of (a) fluorescent pseudomonads (CFU on
663 Gould's S1 medium) and the functional genes (b) *phlD* and (c) *hcnAB* in the rhizosphere of uninfected
664 (white) and infected (grey) plants at the treatment compartments (triangles) and the systemic
665 compartments (squares) of the soil experiment. Regression fits refer to the respective generalized linear
666 model (with gamma distributed errors and a log-link function).



667

668

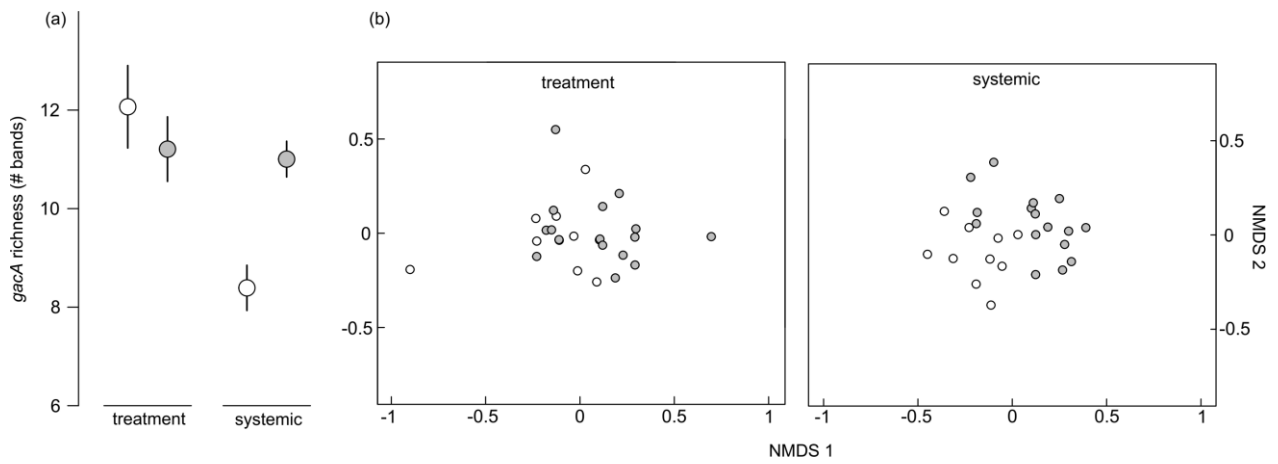
669 **Fig 3** Abundance (least-square means and standard errors) of (a) 16s rDNA and the functional genes (b)
 670 *phlD* and (c) *hcnAB* in the rhizosphere of uninfected plants (white circles, left) and infected plants (grey
 671 circles, right) of the soil experiment. Treatment compartments are paired to the left and the systemic
 672 compartments are paired to the right. For significant infection treatment x compartment side interactions
 673 ($p < 0.1$) additional p-values are given for the pairwise contrasts of the infection treatment within each
 674 compartment side.



675

676

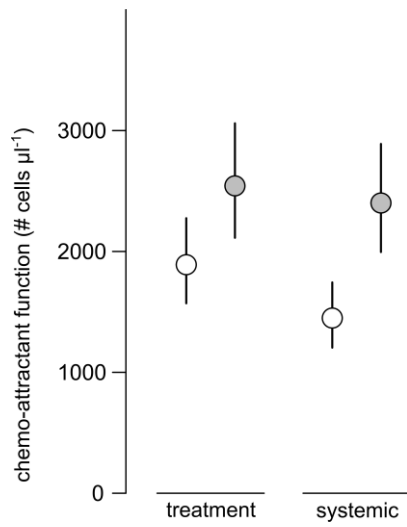
677 **Fig 4** *gacA* allelic richness (a) (least-square means and standard errors) and *gacA* community composition
678 (based on NMDS ordination) (b) in the rhizosphere of uninfected plants (white circles, left) and infected
679 plants (grey circles, right) of the soil experiment. In panel (a) treatment compartments are paired to the left
680 and the systemic compartments are paired to the right. In panel (b) each point represents one single plant.
681 For both compartment sides, the results from the single gel ordinations are superimposed to aid
682 visualization.



683

684

685 **Fig 5** Chemo-attractant function (least-square means and standard errors) of *P. protegens* towards the root
686 exudates of uninfected plants (white circles, left) and infected plants (grey circles, right) of the chemotaxis
687 experiment. Treatment compartments are paired to the left and the systemic compartments are paired to
688 the right.



689